Journal of Macromolecular Science, Part A
Publication details, including instructions for authors and subscription information:
http://www.informaworld.com/smpp/title~content=t713597274

Calculation of the Phase Behavior of Polystyrene Poly(N-Pentyl Methacrylate) Blends

Dieter Browarzik[a]
[a] Institute of Physical Chemistry, Martin-Luther University Halle-Wittenberg, Merseburg, Germany

To cite this Article Browarzik, Dieter(2005) 'Calculation of the Phase Behavior of Polystyrene Poly(N-Pentyl Methacrylate) Blends', Journal of Macromolecular Science, Part A, 42: 10, 1339 — 1353
To link to this Article: DOI: 10.1080/10601320500204858
URL: http://dx.doi.org/10.1080/10601320500204858

Journal of Macromolecular Science®, Part A: Pure and Applied Chemistry, 42:1339–1353, 2005

ISSN 1060-1325 print/1520-5738 online
DOI: 10.1080/10601320500204858

Calculation of the Phase Behavior of Polystyrene + Poly(N-Pentyl Methacrylate) Blends

DIETER BROWARZIK

Institute of Physical Chemistry, Martin-Luther University Halle-Wittenberg, Merseburg, Germany

Polystyrene + poly(n-pentyl methacrylate) blends can show two cloud-point curves. The lower one shows an upper critical solution temperature (UCST) and, the higher one a lower critical solution temperature (LCST). With increasing molar mass of the polystyrene sample both curves become closer and closer to merge, finally by formation of an hour-glass type phase diagram. Based on the Flory-Huggins theory and on continuous thermodynamics the transition of the UCST/LCST behavior into the hour-glass behavior is described in reasonable agreement with the experimental data from the literature. In this paper, the χ-parameter is assumed to be a quadratic polynomial with respect to $1/T$. Furthermore, with the aid of continuous thermodynamics the molar-mass polydispersity in its influence on the phase behavior is theoretically studied.

Keywords polystyrene + poly(n-pentyl methacrylate) blends, Flory-Huggins theory, continuous thermodynamics of polymer blends, phase behavior, polydispersity effects

Introduction

The phase behavior of polymer blends has been investigated extensively both experimentally and theoretically (1–24). Usually, homopolymer blends show either UCST (upper critical solution temperature) behavior or LCST (lower critical solution temperature) behavior. The coexistence of both transitions (UCST at lower temperatures and LCST at higher temperatures) has been known for a long time in the case of a homopolymer solution (1) and for mixtures of a copolymer and a homopolymer (7, 9). However, to the best of my knowledge the occurrence of both types of transition in the same homopolymer mixture has been reported only very recently by Ryu et al. (21) for polystyrene + poly(n-pentyl methacrylate) blends (PS + PnPMA blends). These authors measured the cloud-point curves of some mixtures of this type varying the molar mass of the PS sample. With increasing molar mass of the PS sample, the UCST curve and the LCST curve become closer and closer to finally form hour-glass behavior. The transition of the UCST/LCST behavior into the hour-glass behavior is caused by very small changes of the molar mass of the PS sample. Modelling this impressive phase behavior is an interesting task. Therefore, Voutsas et al. (24) applied the EFV/UNIFAC model, the

Received and Accepted March 2005
Address correspondence to Dieter Browarzik, Institute of Physical Chemistry, Martin-Luther University Halle-Wittenberg, 06217 Merseburg, Germany. E-mail: browarzik@chemie.uni-halle.de

Peng-Robinson equation of state and the Sanchez-Lacombe equation of state to the PS + PnPMA blends mentioned above (24). Surprisingly, only the Sanchez-Lacombe equation of state provided at least a qualitatively (but not quantitatively) correct description of the phase behavior.

In this paper, the Flory-Huggins theory, together with continuous thermodynamics (25–28), proved to be able to describe the experimental phase-equilibrium data (21) reasonably well. Here, the temperature dependence of the parameter χ is assumed to obey the expression $\chi = a + b/T + c/T^2$. The polymer mixtures experimentally studied by Ryu et al. (21) consisted of nearly monodisperse polymer samples. Nevertheless, continuous thermodynamics is needed to describe the very small polydispersity of these mixtures because their phase behavior is extremely sensitive to changes of molar mass. Thus, polydispersity is very important, even in the case of nearly monodisperse polymers. Hence, an interesting question is, how much stronger polydispersities than the experimental ones would influence the phase equilibrium of PS + PnPMA blends. To answer this question is a further goal of this paper. For this purpose, computer simulations based on the parameters previously fitted are performed.

Experimental

Ryu et al. (21) obtained experimental cloud-points for four PS + PnPMA blends exhibiting the transition of UCST/LCST behavior into hour-glass behavior. The following calculations are related to these data. In all mixtures, the polymer B (PnPMA) is characterized by $\bar{M}_n = 7570\,\mathrm{g/mol}$ and $U = 0.0172$ where the non-uniformity U is defined by $U = \bar{M}_w/\bar{M}_n - 1$. $\bar{M}_n$ and $\bar{M}_w$ are the number average and the mass average of the molar mass. The four PS polymer samples are: PS-L ($\bar{M}_n = 6610$; $U = 0.0303$), PS-BL ($\bar{M}_n = 6835$; $U = 0.0268$), PS-BH ($\bar{M}_n = 6960$; $U = 0.0248$) and PS-H ($\bar{M}_n = 7110$; $U = 0.0225$). The samples PS-BL and PS-BH are mixtures of the samples PS-L and PS-H. The mass fractions of PS-H and PS-L are 0.45/0.55 in PS-BL and 0.70/0.30 in PS-BH. The values of the non-uniformity U of the samples PS-BL and PS-BH (given above) were obtained by interpolation according to these mass fractions. Figure 1 shows the experimental phase equilibrium data for the four polymer blends. The blends

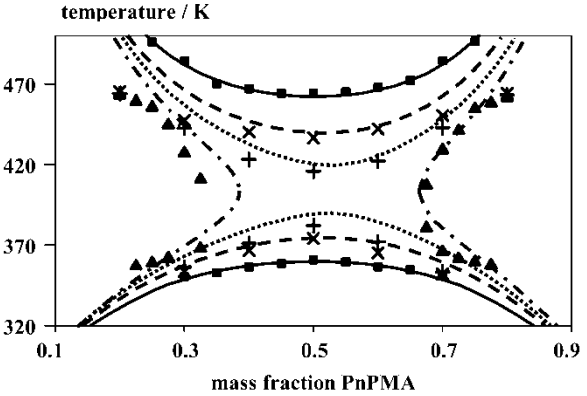

Figure 1. Cloud-point curves of PS + PnPMA blends; calculated: (——) PS-L + PnPMA, (– – –) PS-BL + PnPMA, (·····) PS-BH + PnPMA; (–·–) PS-H + PnPMA; experimental [21]: (■) PS-L + PnPMA, (✗) PS-BL + PnPMA, (+) PS-BH + PnPMA; (▲) PS-H + PnPMA.

PS-L + PnPMA, PS-BL + PnPMA and PS-BH + PnPMA are characterized by UCST/LCST behavior. With increasing molar mass of the PS sample the distance between the UCST curve and the corresponding LCST curve decreases. The blend PS-H + PnPMA is already one of the hour-glass type. The transition of the UCST/LCST type into the hour-glass type happens within the small molar-mass range of $\bar{M}_n = 6960$ and $\bar{M}_n = 7110$.

Results and Discussion

Theoretical Background

Usually, polymers are multicomponent mixtures of similar polymer species differing in molar mass. This polydispersity influences the phase equilibrium of polymer systems in a considerable way. So, instead of a single binodal curve, there are, a cloud-point curve, a so called shadow curve and an infinite number of coexistence curves. The polymer blends considered here are very sensitive to changes of molar mass. Therefore, the polydispersity effects have to be taken into account even in the case of nearly monodisperse polymer samples. To consider the molar-mass polydispersity continuous thermodynamics (25–28) is a powerful tool. Here, a mass distribution function $W(r)$ describes the composition of a polydisperse polymer. Assuming the segment number r to be proportional to the molar mass $W(r)dr$ is the mass fraction of all polymer species with segment numbers between r and $r + dr$. An important advantage of continuous thermodynamics is the essential mathematical and numerical simplification originating from the use of some analytical expressions for the distribution function. One of these expressions is the Schulz-Flory distribution:

$$W(r) = \frac{k^k}{\bar{r}\Gamma(k)}\left(\frac{r}{\bar{r}}\right)^k \exp\left(-k\frac{r}{\bar{r}}\right) \tag{1}$$

Here, $\bar{r}$ is the number average of the segment number being proportional to the number average $\bar{M}_n$ of the molar mass. Γ is the Gamma function. The parameter k describes the width of the distribution and, is related to the non-uniformity U by $k = 1/U$ where, U is defined by:

$$U = \bar{M}_w/\bar{M}_n - 1 \tag{2}$$

Here, $\bar{M}_w$ is the mass average of the molar mass.

In the following a mixture of the polydisperse homopolymers A and B exhibiting a liquid-liquid equilibrium between a bulk phase I and an incipient phase II is considered. Using the Flory-Huggins theory in the framework of continuous thermodynamics the change of the segment-molar Gibbs free energy at mixing may be expressed by:

$$\Delta G_s/RT = \int_0^\infty \frac{\psi_A W_A(r_A)}{r_A}\ln[\psi_A W_A(r_A)] + \int_0^\infty \frac{\psi_B W_B(r_B)}{r_B}\ln[\psi_B W_B(r_B)] + \chi(T)g(\psi_B) \tag{3}$$

Here, $\psi_B = 1 - \psi_A$ is the mass fraction of the polymer B. The integrals describe the entropic effects originating from the size differences of the molecules. The last term with the temperature dependent χ-parameter describes the intermolecular interactions.

In this paper the functions $\chi(T)$ and $g(\psi_B)$ are assumed to obey:

$$\chi = A + B/T + C/T^2 \tag{4a}$$

$$g(\psi_B) = \psi_B(1-\psi_B)[1 + \alpha\psi_B + \beta(\psi_B)^2] \tag{4b}$$

Furthermore, both polymers in the phase I are assumed to obey the Schulz-Flory distribution. Doing so and, applying continuous thermodynamics (25, 26) the distribution functions of the polymers A and B in the phase II prove to be Schulz-Flory distributions as well. Furthermore, the parameters k_A and, respectively, k_B take the same values in both phases and, the number averages of the segment numbers in the phase II are given by:

$$\frac{1}{\bar{r}_A^{II}} = \frac{1}{\bar{r}_A^{I}}\left(\frac{1-\psi_B^I}{1-\psi_B^{II}}\right)^{\frac{1}{k_A+1}}; \quad \frac{1}{\bar{r}_B^{II}} = \frac{1}{\bar{r}_B^{I}}\left(\frac{\psi_B^I}{\psi_B^{II}}\right)^{\frac{1}{k_B+1}} \tag{5}$$

Here, ψ_B^I and ψ_B^{II} are the total mass fractions of the polymer B in the given phase I and the incipient phase II. The phase equilibrium conditions result in two equations permitting the calculation of the two unknowns ψ_B^{II} and χ (for details see (25, 26):

$$\begin{aligned} 0 = {} & \frac{k_A}{\bar{r}_A^I}\left[1 - \left(\frac{1-\psi_B^{II}}{1-\psi_B^I}\right)^{-\frac{1}{k_A+1}}\right] + \frac{1-\psi_B^I}{\bar{r}_B^I}\left[1 - \left(\frac{1-\psi_B^{II}}{1-\psi_B^I}\right)^{\frac{k_A}{k_A+1}}\right] \\ & + \frac{\psi_B^I}{\bar{r}_B^I}\left[1 - \left(\frac{\psi_B^{II}}{\psi_B^I}\right)^{\frac{k_B}{k_B+1}}\right] \\ & + \chi(T)\left[\left(g - \psi_B\frac{dg}{d\psi_B}\right)^{II} - \left(g - \psi_B\frac{dg}{d\psi_B}\right)^{I}\right] \end{aligned} \tag{6a}$$

$$\begin{aligned} \chi(T) = {} & \left\{\frac{k_B}{\bar{r}_B^I}\left[1 - \left(\frac{\psi_B^{II}}{\psi_B^I}\right)\right]^{-\frac{1}{k_B+1}} - \frac{k_A}{\bar{r}_A^I}\left[1 - \left(\frac{1-\psi_B^{II}}{1-\psi_B^I}\right)^{-\frac{1}{k_A+1}}\right]\right\} \\ & \cdot \left[\left(\frac{dg}{d\psi_B}\right)^{I} - \left(\frac{dg}{d\psi_B}\right)^{II}\right]^{-1} \end{aligned} \tag{6b}$$

To obtain ψ_B^{II}, one has to solve numerically Equation (6a) taking χ from Equation (6b). Knowing ψ_B^{II}, the parameter χ may be calculated in a straight forward way by Equation (6b). With the aid of Equation (4a), the temperature T may be calculated by:

$$T = \frac{2C}{-B \pm \sqrt{B^2 + 4C(\chi - A)}}; \quad B^2 + 4C(\chi - A) \geq 0 \tag{7}$$

So, the cloud-point curve $T(\psi_B^I)$ and the so-called shadow curve $T(\psi_B^{II})$ may be calculated. The shadow curve characterizes the incipient phase II and is experimentally available only by extrapolation of the coexistence curves. Cloud-point curve and shadow curve coincide only in the critical point, which is usually, the intersection point of both curves.

In addition to the calculation of these curves, often the knowledge of the spinodal curve and of the critical point is important. To obtain information about these quantities, the stability theory of continuous thermodynamics (27) has to be applied. The most fundamental quantity in this treatment is the second order differential $\delta^2 G_s$ of the segment-molar

Gibbs free energy. Finding the variations, δW_A^*, δW_B^*, which minimize $\delta^2 G_s$ and setting the minimum equal to zero the spinodal condition is obtained. The details of this mathematical procedure were outlined in a previous paper (27) related to polymer solutions. The case of a polymer mixture may be analogously treated. According to that the spinodal condition reads:

$$0 = \frac{k_A}{\bar{r}_A(k_A+1)(1-\psi_B)} + \frac{k_B}{\bar{r}_B(k_B+1)\psi_B} + \chi(T)\frac{d^2g}{d\psi_B^2} \tag{8}$$

Equations (7) and (8) permit the calculation of the spinodal temperature in a straightforward way. Usually, in the polydisperse case, the extreme value of the spinodal curve does not coincide with the extreme values of the cloud-point curve or of the shadow curve. Forming the first differential of the spinodal condition, introducing the minimizing variations δW_A^*, δW_B^* and, setting the obtained expression equal to zero a second necessary condition for the critical point is obtained. Based on the Schulz-Flory distribution (1) this condition is:

$$0 = \frac{1}{\bar{r}_A}\frac{k_A(k_A+2)}{(k_A+1)^2}\frac{1}{(1-\psi_B)^2} - \frac{1}{\bar{r}_B}\frac{k_B(k_B+2)}{(k_B+1)^2}\frac{1}{(\psi_B)^2} + \chi(T)\frac{d^3g}{d\psi_B^3} \tag{9}$$

Combining Equations (8) and (9) $\chi(T)$ may be eliminated and the numerical solution of the resulting equation yields the critical mass fraction $\psi_{B,cr}$. The corresponding quantities χ_{cr} and T_{cr} may be directly calculated with the aid of Equations (7) and (8). Usually, in the polydisperse case the critical point is different from the extreme values of the cloud-point curve, of the shadow curve and of the spinodal curve. In the critical point the cloud-point curve and the spinodal curve possess the same slope.

Comparison of Theory and Experiment

The following calculations relate to the experimental data of Ryu et al. (21). The phase behaviour of the blends PS-L + PnPMA, PS-BL + PnPMA, PS-BH + PnPMA and PS-H + PnPMA is considered. The characterization data of the polymers are listed in the experimental section. Figure 1 shows the experimental phase-equilibrium data. In the calculations the monomer unit of polystyrene was chosen as reference segment. The segment number is considered to be proportional to the molar mass. Then, using the values of $\bar{M}_n$ and U the parameters $\bar{r}$ and k are also known. The parameters A, B, C of Equation (4a) were fitted to the experimental cloud-points at $\psi_B = 0.5$ of the blends, PS-L + PnPMA, PS-BL + PnPMA and PS-BH + PnPMA. The parameters α, β of Equation (4b) were fitted to all experimental cloud-points of the blend PS-L + PnPMA. The values obtained in this way are:

$$A = 0.094871;\ B = -48.8601;$$
$$C = 9884.59\ K^2 \text{ and } \alpha = -0.3736;\ \beta = 0.401.$$

Using these values, the cloud-point curves for all four polymer blends mentioned above were calculated. The agreement with the experimental values is reasonably good as Figure 1 shows. Especially, the curves of the mixture PS-L + PnPMA are described nearly quite perfect. Of course, this is not a surprise because the parameters α, β were fitted to the experimental data of this mixture. However, the prediction of the hour-glass shaped curves (PS-H + PnPMA) is also reasonably well (none of the

experimental data of this system were included in the parameter fit). Somewhat larger deviations from the experimental values occur only in the LCST curves of the blends PS-BL + PnPMA and PS-BH + PnPMA. These curves are a little too small. Nevertheless, the agreement between the calculated curves and the experimental points is generally better than in the case of the much more complicated Sanchez-Lacombe equation applied by Voutsas et al. (24).

Influence of Polydispersity on Phase Behavior

For the liquid-liquid equilibrium of PS/methyl cyclohexane solutions, the influence of polydispersity on the pressure-concentration diagram has been reported previously (29, 30). Here, the influence of polydispersity on the temperature-concentration diagram of PS + PnPMA blends is to be discussed. Because experimental data are not available, computer simulations based on Equations (6–9) have to be performed. The basic data set is taken from PS-BH + PnPMA. Firstly, $\bar{M}_n$ (respectively $\bar{r}$) is fixed for both polymers and, the non-uniformities U (respectively $\bar{M}_w$ and k) are changed. Therefore, in Figures 2–10, $\bar{M}_{n,A} = 6960\,\mathrm{g/mol}$; $\bar{M}_{n,B} = 7570\,\mathrm{g/mol}$ is assumed.

In Figure 2, the monodisperse case $U_A = 0$; $U_B = 0$ is considered. Here, the UCST curve and the LCST curve show a larger distance from each other than in the case of the real system PS-BH + PnPMA (see Figure 1). So, the monodisperse polymers are better miscible than the polydisperse ones.

In the case $U_A = 0.05$; $U_B = 0.05$ (Figure 3) hour-glass behavior is already found. This example shows that at fixed number average of the molar mass very small changes of the non-uniformity U (or respectively of $\bar{M}_w$) essentially influence the phase behaviour. Instead of the two binodal curves of the monodisperse case here, there are the two cloud-point curves (full lines) 1 and 2 and the shadow curves (dashed lines) 1* (corresponding to 1) and 2* (corresponding to 2). The shadow curves describe the equilibrium temperature as function of the concentration of the incipient phase II (that corresponds to the bulk phase I). In the monodisperse case, the curves 1 and 2* coincide and, the curves 2 and 1* do as well. Because of the small non-uniformity, the cloud-point curve 1 and the shadow curve 2* and, respectively, the cloud-point curve 2 and the shadow curve 1* are very similar to each other. Different from Figure 2, there

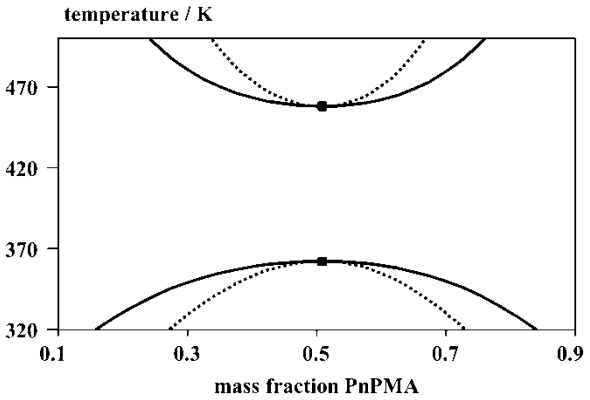

Figure 2. Calculated cloud-point curves (——), spinodal curves (·····) and critical points (■) for a monodisperse mixture ($U_A = U_B = 0$) with $\bar{M}_{n,A} = 6960\,\mathrm{g/mol}$ and $\bar{M}_{n,B} = 7570\,\mathrm{g/mol}$.

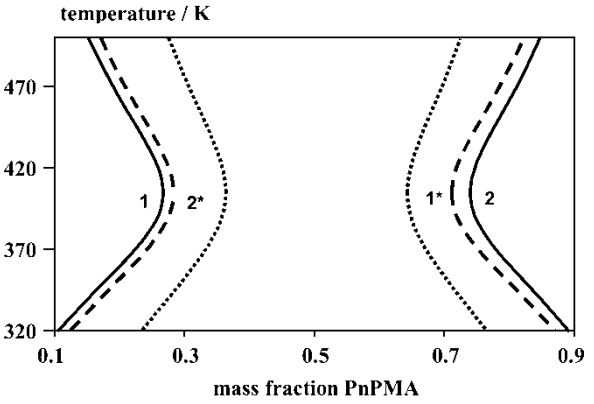

Figure 3. Calculated cloud-point curves (——), shadow curves (– – –) and spinodal curves (·····) for a polydisperse mixture with $U_A = U_B = 0.05$ and the same number averages as in Figure 2.

are no critical points. Contrary to the UCST/LCST type, the hour-glass shaped cloud-point curves surround the miscibility region.

Figure 4 shows the effect if only the polymer B is polydisperse ($U_A = 0$; $U_B = 0.05$). Here, the cloud-point curves show already hour-glass behavior. However, the spinodal curves (dotted lines) are still of the UCST/LCST type. Different from Figure 3 there are two critical points on the cloud-point curve 2 (full line) being the intersection points of this cloud-point curve and the corresponding shadow curve 2* (dashed line). The cloud-point curve 1 and the shadow curve 1* have no critical point in common and therefore, they are very distant from each other. The cloud-point curve 1 (respectively 2) and the shadow curve 2* (respectively 1*), which would coincide in the monodisperse case, are very different although only the polymer B shows a very small polydispersity. In the critical points in each case one spinodal curve and the cloud-point curve 2 touch with the same slope. In Figure 5, the opposite case to Figure 4 with a polydisperse polymer A ($U_A = 0.045$) and a monodisperse polymer B ($U_B = 0$) is considered. Therefore, Figure 5 is very similar to Figure 4 however with an opposite symmetry.

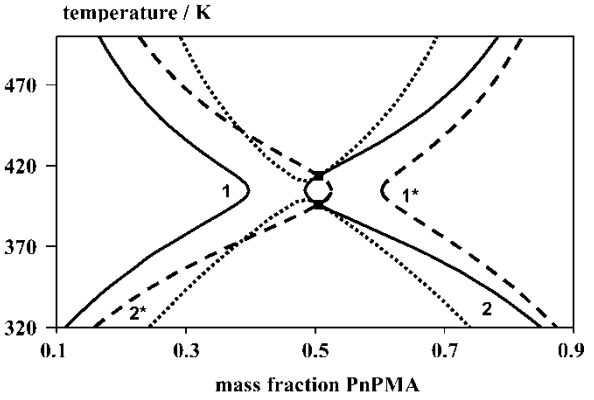

Figure 4. Calculated cloud-point curves (——), shadow curves (– – –), spinodal curves (·····) and critical points (■) for a polydisperse mixture with $U_A = 0$; $U_B = 0.05$ and the same number averages as in Figure 2.

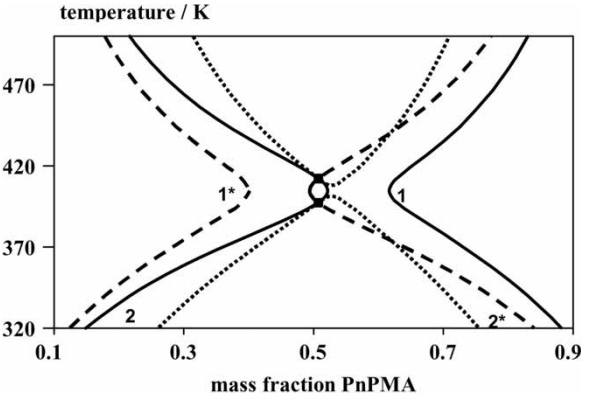

Figure 5. Calculated cloud-point curves (——), shadow curves (– – –), spinodal curves (·····) and critical points (■) for a polydisperse mixture with $U_A = 0.045$; $U_B = 0$ and the same number averages as in Figure 2.

The cases with only one of the polymers being polydisperse (Figures 4 and 5) seem to be particularly interesting. For this reason, in the next case, $U_A = 0$; $U_B \neq 0$ for some values of U_B is to be considered more in detail. Let us start with the case $U_A = 0$; $U_B = 0.048$. Here, the cloud-point curves and the spinodal curves still show UCST/LCST behavior (Figure 6). The extreme values of the cloud-point curves (and respectively of the shadow curves) are already very close to each other. Increasing the polydispersity of the polymer B ($U_A = 0$; $U_B = 0.04868$) the cloud-point curves 1 and 2 (and the shadow curves 1^* and 2^*) coincide forming a cross (Figure 7). A further increase of the polydispersity U_B leads to hour-glass behavior of the cloud-point curves as shown in Figure 4 ($U_A = 0$; $U_B = 0.05$). For $U_A = 0$; $U_B = 0.05080$ the spinodal curves coincide forming a cross (Figure 8). The critical points do still exist. For higher values than $U_B = 0.05080$, the spinodal curves show hour-glass behavior as the cloud-point curves already do. For $U_A = 0$; $U_B = 0.05186$, the critical points merge (Figure 9). The cloud-point curve 2, the shadow curve 2^* and one of the spinodal curves coincide in this one

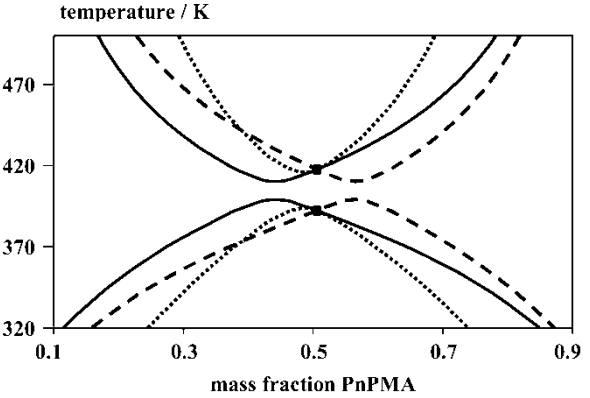

Figure 6. Calculated cloud-point curves (——), shadow curves (– – –), spinodal curves (·····) and critical points (■) for a polydisperse mixture with $U_A = 0$; $U_B = 0.048$ and the same number averages as in Figure 2.

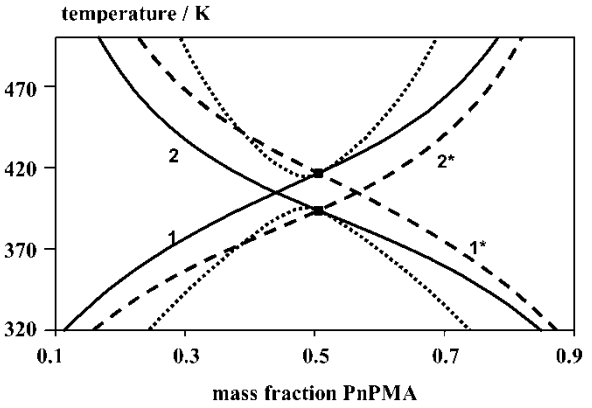

Figure 7. Calculated cloud-point curves (——), shadow curves (– – –), spinodal curves (·····) and critical points (■) for a polydisperse mixture with $U_A = 0$; $U_B = 0.04868$ and the same number averages as in Figure 2; the cloud-point curves show the transition from the UCST/LCST behavior into the hour-glass behavior.

critical point. In Figure10, the case $U_A = 0$; $U_B = 0.1$ is presented. All curves show hour-glass behavior. The cloud-point curves touch neither the corresponding shadow curves nor the spinodal curves. Critical points no longer exist.

One can change the non-uniformity U also by varying the number average $\bar{M}_n$ of the molar mass at constant mass average $\bar{M}_w$. According to Equations (2) and (8) (with $k = 1/U$) the spinodal curve is independent of U in this case. The critical points depend slightly on the non-uniformity U.Therefore, mainly the cloud-point curves (and the shadow curves) are influenced by the polydispersity. For this reason, such a consideration may be expected to be very interesting. Let us consider the mixture PS-BH + PnPMA with $\bar{M}_{w,A} = 7133$; $\bar{M}_{w,B} = 7700$ (in g/mol) to be the reference system again. These mass averages correspond to the number averages $\bar{M}_n$ and the non-uniformities U of the real samples PS-BH and PnPMA as outlined before. Starting with the case, $U_A = U_B = 0$,

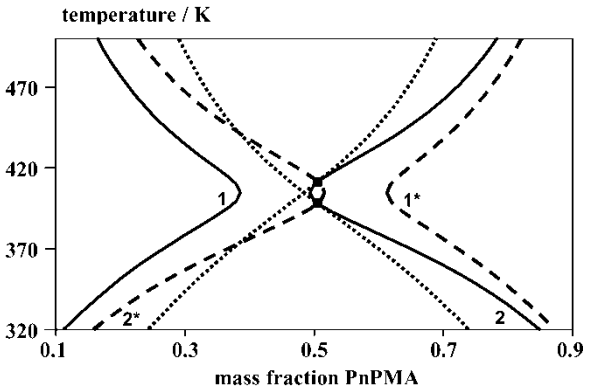

Figure 8. Calculated cloud-point curves (——), shadow curves (– – –), spinodal curves (·····) and critical points (■) for a polydisperse mixture with $U_A = 0$; $U_B = 0.05080$ and the same number averages as in Figure 2; the spinodal curves show the transition from the UCST/LCST behaviour into the hour-glass behavior.

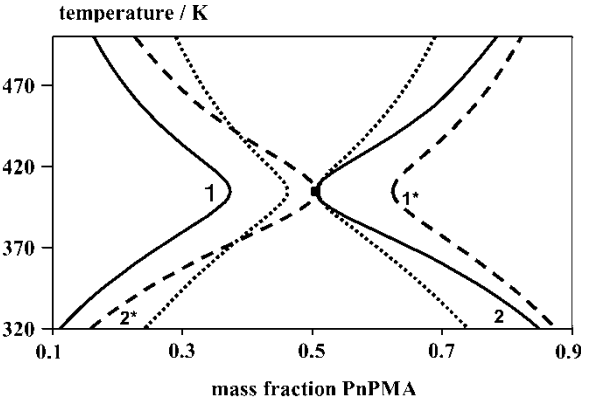

Figure 9. Calculated cloud-point curves (—), shadow curves (---), spinodal curves (·····) and critical point (■) for a polydisperse mixture with $U_A = 0$; $U_B = 0.05186$ and the same number averages as in Figure 2; coincidence of the two critical points.

an UCST/LCST behavior with the critical temperatures 389.60 K and 420.82 K is found. The phase diagram is similar to that of Figure 2 except for the difference between the both critical temperatures, which is lower than in Figure 2 (because of the higher number averages $\bar{M}_n = \bar{M}_w$). Increasing only U_B, the cloud-point curves become closer and closer to coincide and form hour-glass behavior. Then (at $U_B = 0.1$ for instance), the phase diagram is similar to Figure 4. Of course, as an important difference to Figure 4, the spinodal curve is the same as in the corresponding monodisperse polymer mixture. As particularity, the critical concentration $\psi_{B,\mathrm{cr}}$ of the polymer B shifts slightly to higher values. If one incraseses only U_A at $U_B = 0$, the phase diagram (at $U_A = 0.1$ for instance) is similar to Figure 5. The critical concentration $\psi_{B,cr}$ of the polymer B shifts slightly to lower values. So, all these cases are not worth discussing in further detail because there are no new types of phase diagrams.

However, the simultaneous increase of the non-uniformity U of both polymers results in interesting phase diagrams. Differing from the mixtures previously discussed here, somewhat more polydispersity is required to cause considerable effects. Figure 11

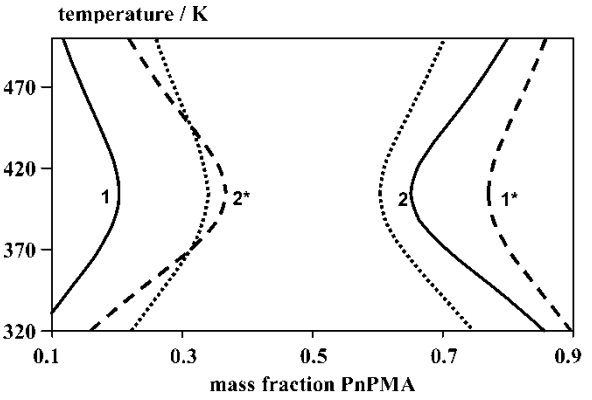

Figure 10. Calculated cloud-point curves (——), shadow curves (– – –) and spinodal curves (·····) for a polydisperse mixture with $U_A = 0$; $U_B = 0.1$ and the same number averages as in Figure 2.

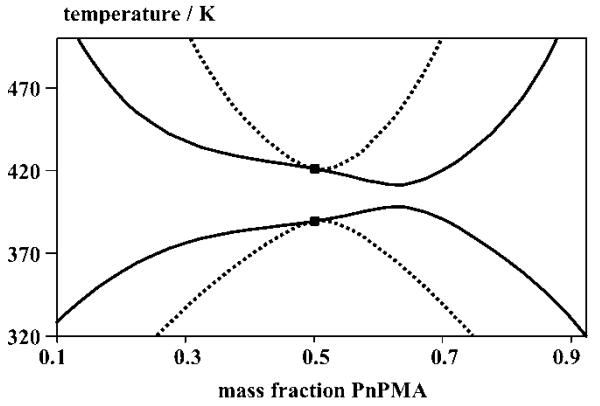

Figure 11. Calculated cloud-point curves (——), spinodal curves (·····) and critical points (■) for a polydisperse mixture with $U_A = U_B = 0.35$ and with $\bar{M}_{w,A} = 7133\,\mathrm{g/mol}$ and $\bar{M}_{w,B} = 7700\,\mathrm{g/mol}$.

presents the phase diagram related to $U_A = U_B = 0.35$. The mass averages here and in the following cases are again $\bar{M}_{w,A} = 7133$; $\bar{M}_{w,B} = 7700$ (in g/mol). For the sake of simplicity, Figure 11 restricts the cloud-point curves (full lines), the spinodal curves (dotted lines) and the critical points. Of course, the spinodal curves in Figure 11 (and in the following figures) are the same as in the monodisperse case. Generally, in the case $U_A = U_B$, the change of the critical points related to the corresponding monodisperse mixture is only very small. In Figure 11, the extreme values of the cloud-point curves are very close to each other and differ considerably from the critical points. Figure 12 shows the effect of further increase of polydispersity ($U_A = U_B = 0.4$). Instead of the UCST/LCST curves of Figure 11 here, hour-glass shaped curves occur. The cloud-point curves surround the miscibility regions. The increase of polydispersity leads to a decrease of miscibility. At $U_A = U_B = 0.85$ (Figure 13) on the left cloud-point curve two additional extreme values occur, giving this curve the shape of a fish. With a further increase of polydispersity, these two extreme values become closer and closer, coincide, and a separate closed cloud-point curve in the middle part of the diagram is formed ($U_A = U_B = 0.9$; Figure 14). Different from the usual closed-loop phase

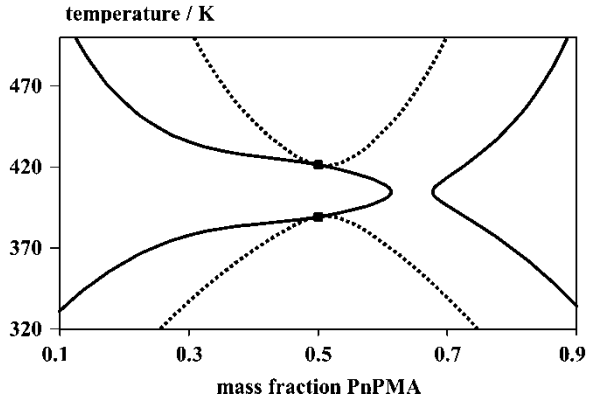

Figure 12. Calculated cloud-point curves (——), spinodal curves (·····) and critical points (■) for a polydisperse mixture with $U_A = U_B = 0.4$ and the same mass averages as in Figure 11.

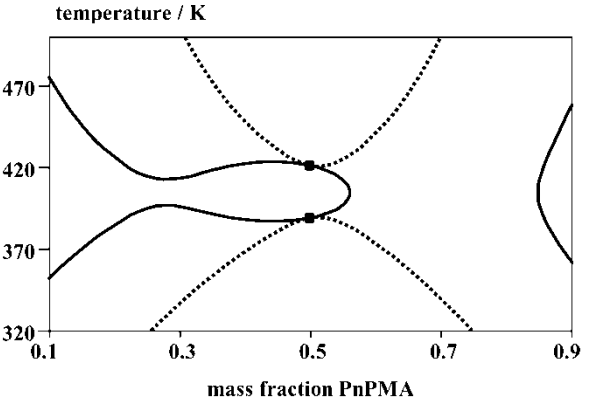

Figure 13. Calculated cloud-point curves (——), spinodal curves (·····) and critical points (■) for a polydisperse mixture with $U_A = U_B = 0.85$ and the same mass averages as in Figure 11.

behavior, the miscible region is inside of the cloud-point curve (miscibility island). So, there are three cloud-point curves surrounding miscible regions. One reason for this curious behavior is the fixed mass averages $\bar{M}_{w,A}$, $\bar{M}_{w,B}$. Therefore, the spinodal curves cannot change with polydispersity. Another reason is the equality of the polydispersities of both polymers. So, the position of the critical points is nearly independent of the polydispersity. Because the critical points are always located on a cloud-point curve a miscibility island remains even if the values of $U_A = U_B$ increase. Figures 11–14 do not contain the shadow curves because there are no particularities additionally to Figures 3–10. However, in the case of the miscibility island of Figure 14, it is interesting to also discuss the shadow curve. This is illustrated by Figure 15, but only focussed to the middle part of the phase diagram containing the miscibility island. Therefore, Figure 15 is restricted to only this one cloud-point curve, the corresponding shadow curve, the spinodal curves and the critical points. For the sake of clearness, it has to be noted that a cloud-point and the corresponding shadow point are generally located on different sides of the critical points.

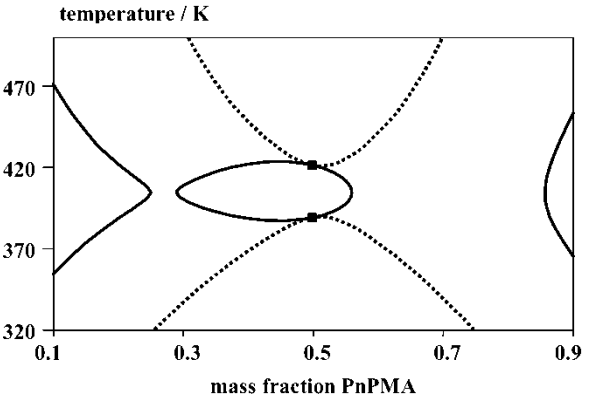

Figure 14. Calculated cloud-point curves (——), spinodal curves (·····) and critical points (■)for a polydisperse mixture with $U_A = U_B = 0.9$ and the same mass averages as in Figure 11; occurrence of a miscibility island.

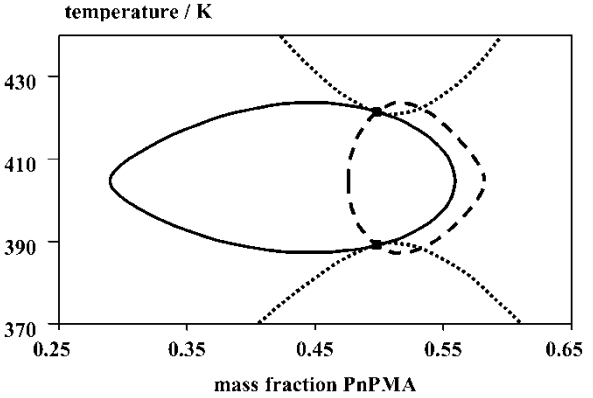

Figure 15. Calculated cloud-point curves (——), shadow curves (– – –), spinodal curves (·····) and critical points (■) for the same mixture as in Figure 14 but, focussed to the region of the miscibility island.

Conclusions

Polystyrene + poly(n-pentyl methacrylate) blends can show UCST/LCST behavior and hour-glass behavior. With increasing molar mass of the PS samples there is a transition of the UCST/LCST behavior into the hour-glass behavior. The Flory-Huggins theory together with continuous thermodynamics is able to describe this transition if the parameter χ is assumed to be a quadratic polynomial with respect to $1/T$. The agreement of the calculated results and the experimental data of Ryu et al. (21) is reasonably good. The molar-mass polydispersity strongly influences the phase equilibrium. Fixing the number average $\bar{M}_n$ even very small non-uniformities (e.g. $U = 0.05$) result in an essential change of the phase behavior. In the case of a mixture of a monodisperse polymer and a polydisperse polymer with increasing non-uniformity U, firstly, the cloud-point curves coincide to form hour-glass behavior. With further increasing values of, U the spinodal curves coincide and form hour-glass shaped curves too. At this stage, there are still critical points, which vanish only at more polydispersity. Fixing the mass average $\bar{M}_w$ the spinodal curves do not depend on polydispersity. In the particularly interesting case $U_A = U_B$ the critical points are also nearly independent of polydispersity. So with increasing polydispersity only the cloud-point curves (and, respectively, the shadow curves) change. In this, the cloud-point curves firstly coincide at their extreme values changing into hour-glass shaped curves. For stronger polydispersity, two additional extreme values are formed on one of the cloud-point curves. Finally, by coincidence of these extreme values a closed cloud-point curve (respectively shadow curve) is formed. The miscible region is inside and the immiscible region is outside of this cloud-point curve (island miscibility).

References

1. Saeki, S., Kuwahara, N., Konno, S., and Kaneko, M. (1973) Upper and Lower Critical Solution Temperatures in Polystyrene Solutions. *Macromolecules*, 6 (2): 246–250.
2. McMaster, L.P. (1973) Polymer-Polymer Thermodynamics. *Macromolecules*, 6 (5): 760–773.
3. Paul, D.R. and Newman, S. eds.: (1978) *Polymer Blends*; Academic Press: New York.

4. Patterson, D. and Robard, A. (1978) Thermodynamics of Polymer Compatibility. *Macromolecules*, 11 (4): 690–695.
5. Sanchez, I.C. and Lacombe, R.H. (1978) Statistical Thermodynamics of Polymer Solutions. *Macromolecules*, 11 (6): 1145–1156.
6. Sanchez, I.C. (1982) *Polymer Compatibility and Incompatibility*; Solc, K., ed.; MMI Press: New York.
7. Ougizawa, T., Inoue, T., and Kammer, H.W. (1985) UCST and LCST Behavior in Polymer Blends. *Macromolecules*, 18 (10): 2089–2092.
8. Bates, F.S., Wignall, G.D., and Koehler, D.K. (1985) Critical Behavior of Binary Liquid Mixtures of Deuterated and Protonated Polymers. *Phys. Rev. Lett.*, 55 (22): 2425–2428.
9. Cong, G., Huang, Y., MacKnight, W.J., and Karasz, F.E. (1986) Upper and Lower Critical Solution Temperature Behavior in Thermoplastic Polymer Blends. *Macromolecules*, 19 (11): 2765–2770.
10. Dudowicz, J. and Freed, K.F. (1991) Effect of Monomer Structure and Compressibility on the Properties of Multicomponent Polymer Blends and Solutions: 1. Lattice Cluster Theory of Compressible Systems. *Macromolecules*, 24 (18): 5076–5095.
11. Dudowicz, J. and Freed, K.F. (1993) Relation of Effective Interaction Parameters for Binary Blends and Diblock Copolymers: Lattice Cluster Theory Predictions and Comparisons with Experiment. *Macromolecules*, 26 (1): 213–220.
12. Hammouda, B., Bauer, B.J., and Russell, T.P. (1994) Small-Angle Neutron Scattering from Deuterated Polystyrene/Poly(Butyl Methylacrylate) Homopolymer Blend Mixtures. *Macromolecules*, 27 (8): 2357–2359.
13. Russell, T.P., Karis, T.E., Gallot, Y., and Mayes, A.M. (1994) A Lower Critical Ordering Transition in a Diblock Copolymer Melt. *Nature (London)*, 368 (6473): 729–731.
14. Graessley, W.W., Krishnamoorti, R., Reichart, G.C., Balsara, N.P., Fetters, L.J., and Lohse, D.J. (1995) Regular and Irregular Mixing in Blends of Saturated Hydrocarbon Polymers. *Macromolecules*, 28 (4): 1260–1270.
15. Balsara, N.P. (1997) *Physical Properties of Polymers Handbook (Chapter 19)*; Mark, J.E., ed.; AIP Press: Secaucus, NJ.
16. Hino, T. and Prausnitz, J.M. (1998) Lower and Upper Critical Ordering Temperatures in Compressible Diblock Copolymer Melts from a Perturbed Hard-Sphere-Chain Equation of State. *Macromolecules*, 31 (8): 2636–2648.
17. Cho, J. (2000) Analysis of Phase Separation in Compressible Polymer Blends and Block Copolymers. *Macromolecules*, 33 (6): 2228–2241.
18. Ruzette, A.V.G. and Mayes, A.M. (2001) A Simple Free Energy Model for Weakly Interacting Polymer Blends. *Macromolecules*, 34 (6): 1894–1907.
19. Ruzette, A.V.G., Banerjee, P., Mayes, A.M., Pollard, M., and Russell, T.P. (2001) A Simple Model for Baroplastic Behavior in Block Copolymer Melts. *J. Chem. Phys.*, 114 (8): 8205–8209.
20. Koningsveld, R., Stockmayer, W.H., and Nies, E. (2001) *Polymer Phase Diagram*; Oxford University Press: New York.
21. Ryu, D.Y., Park, M.S., Chae, S.H., Jang, J., Kim, J.K., and Russell, T.P. (2002) Phase Behavior of Poylstyrene and Poly(n-Pentyl Methacrylate) Blend. *Macromolecules*, 35 (23): 8676–8680.
22. Ryu, D.Y., Jeong, U., Lee, D.H., Kim, J., Youn, H.S., and Kim, J.K. (2003) Phase Behavior of Deuterated Polystyrene-Block-Poly(n-Pentyl Methacrylate) Copolymers. *Macromolecules*, 36 (8): 2894–2902.
23. Ryu, D.Y., Lee, D.H., Jeong, U., Yun, S.-H., Park, S., Kwon, K., Sohn, B.-H., Chang, T., Kim, J.K., and Russell, T.P. (2004) Closed-Loop Phase Behavior of Polystyrene-Block-Poly(n-Pentyl Methacrylate) Copolymers with Various Block Length Ratios. *Macromolecules*, 37 (10): 3717–3724.
24. Voutsas, E.C., Pappa, G.D., Boukouvalas, C.J., Magoulas, K., and Tassios, D.P. (2004) Miscibility in Binary Polymer Blends: Correlation and Prediction. *Ind. Eng. Chem. Res.*, 43 (5): 1312–1321.

25. Rätzsch, M.T. and Kehlen, H. (1989) Continuous Thermodynamics of Polymer Systems. *Prog. Polym. Sci.*, 14: 1–46.
26. Browarzik, D., Kehlen, H., Rätzsch, M.T., and Thieme, D. (1988) Liquid-Liquid Equilibrium of Oligomeric Poly(Dimethylsiloxane) + Poly(Dimethyldiphenyl-siloxane) Mixtures. *Acta Polymerica*, 39 (12): 687–691.
27. Browarzik, D., Kehlen, H., and Rätzsch, M.T. (1990) Application of Continuous Thermodynamics to the Stability of Polymer Systems.III. *J. Macromol. Sci.-Chem.*, A27 (5): 549–561.
28. Cotterman, R.L. and Prausnitz, J.M. (1991) Continuous Thermodynamics for Phase Equilibrium Calculations in Process Design. In *Kinetic and Thermodynamic Lumping of Multicomponent Mixtures (229–276)*; Astarita, G. and Sandler, S.I., eds.; Elsevier: Amsterdam.
29. Browarzik, D. and Kowalewski, M. (2002) Calculation of the Cloud-Point and the Spinodal Curve for the System Methylcylohexane/Polystyrene at High Pressures. *Fluid Phase Equilib.*, 194: 451–467.
30. Browarzik, D. and Kowalewski, M. (2004) Calculation of the Stability and of the Phase Equilibrium of the System Methylcylohexane + Polystyrene Based on an Equation of State. In *Thermodynamic Properties of Complex Fluid Mixtures (488–508)*; Maurer, G., ed.; Wiley-VCH: Weinheim.